J Biomol NMR (2009) 44:77–86
DOI 10.1007/s10858-009-9322-2

ARTICLE

Refolding of ribonuclease A monitored by real-time photo-CIDNP NMR spectroscopy

Iain J. Day · Kiminori Maeda · Howard J. Paisley · K. Hun Mok · P. J. Hore

Received: 12 January 2009 / Accepted: 21 April 2009 / Published online: 13 May 2009

Abstract Photo-CIDNP NMR spectroscopy is a powerful method for investigating the solvent accessibility of histidine, tyrosine and tryptophan residues in a protein. When coupled to real-time NMR, this technique allows changes in the environments of these residues to be used as a probe of protein folding. In this paper we describe experiments performed to monitor the refolding of ribonuclease A following dilution from a high concentration of chemical denaturant. These experiments provide a good example of the utility of this technique which provides information that is difficult to obtain by other biophysical methods. Real-time photo-CIDNP measurements yield residue-specific kinetic data pertaining to the folding reaction, interpreted in terms of current knowledge of the folding of bovine pancreatic ribonuclease A.

Keywords Photo-CIDNP · Real-time NMR · Protein folding · Ribonuclease A

I. J. Day · K. Maeda · H. J. Paisley · K. H. Mok (✉) · P. J. Hore (✉)
Department of Chemistry, Physical and Theoretical Chemistry Laboratory, University of Oxford, South Parks Road, Oxford OX1 3QZ, UK
e-mail: mok1@tcd.ie

P. J. Hore
e-mail: peter.hore@chem.ox.ac.uk

Present Address:
I. J. Day
Department of Chemistry and Biochemistry, School of Life Sciences, University of Sussex, Falmer, Brighton BN1 9QJ, UK

Present Address:
K. H. Mok
Trinity College, School of Biochemistry and Immunology, University of Dublin, Dublin 2, Ireland

Introduction

Ribonuclease A (RNase A) is one of the classic proteins used in the investigation of protein folding. It was the first protein to be studied by NMR (Saunders et al. 1957), and was used by Anfinsen in 1973 to demonstrate for the first time that the native three-dimensional fold of a protein is coded purely by its amino acid sequence (Anfinsen 1973). Since this time, it has been the subject of countless studies by protein biochemists and molecular biophysicists interested in how a protein adopts its native three-dimensional structure following synthesis on the ribosome (Neira and Rico 1997; Raines 1998; Narayan et al. 2000; Wedemeyer et al. 2000; Chatani and Hayashi 2001; Dobson 2003). Despite this longstanding and exhaustive body of work, interest in RNase A is still very active. Recently, its misfolding and refolding have been exploited to design a domain-swapped, enzymatically-active fibril in which the engineered monomers are one-dimensionally extended along the fibril axis (Sambashivan et al. 2005). In addition, the RNase A homologue, onconase, is currently in clinical trials for treatment of certain lung cancers, and as a result the oxidative folding of the two proteins is being studied comparatively (Gahl et al. 2008).

Bovine pancreatic RNase A consists of 124 amino acid residues (molecular weight: 14.2 kDa). The structure comprises three α-helices which act as a scaffold for a β-sheet region which contains the active site in a central cleft. The overall topology of the protein is stabilised by the presence of four disulphide bridges, between residues 26–84, 40–95, 58–110, and 65–72. Figure 1 shows the three-dimensional structure as determined by NMR spectroscopy (Santoro et al. 1993). RNase A contains four proline residues, of which two are present as *cis* X-prolyl peptide bonds in the native state. These *cis*-Pro peptide

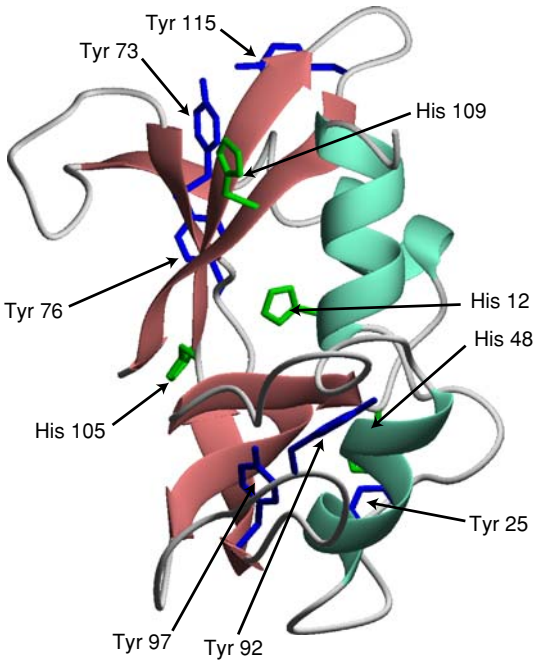

Fig. 1 The NMR structure of bovine pancreatic RNase A (PDB File: 2AAS (Santoro et al. 1993). The potentially CIDNP-observable residues are highlighted, with tyrosine shown in blue and histidine in green. The figure was drawn using MOLMOL (Koradi et al. 1996) and rendered using POVRAY (http://www.povray.org)

bonds precede residues Pro 93 and Pro 114. Both of these residues have been shown to be important to the folding properties of RNase A (Lin and Brandts 1983a, b; Schultz and Baldwin 1992; Schultz et al. 1992; Houry et al. 1994).

The folding of RNase A is currently thought to progress through at least five pathways, with differing, non-native, configurations of *cis* and *trans* X-prolyl peptide bonds (Neira and Rico 1997; Schultz and Baldwin 1992; Schultz et al. 1992; Dodge and Scheraga 1996). Two of these pathways, known as the U_S^I and U_S^{II} phases, proceed through a number of kinetic intermediates. One of these intermediates, I_N, is known to possess native-like structure, in that it maintains some enzymatic activity as monitored by the binding of 2′-cytosine monophosphate (Biringer et al. 1988).

The majority of techniques used to probe protein folding, for example circular dichroism, intrinsic fluorescence and H/D exchange, either provide information on the global folding properties, or on processes occurring at the polypeptide backbone. Photo-Chemically Induced Dynamic Nuclear Polarization (photo-CIDNP) NMR spectroscopy, by contrast, is uniquely placed to provide residue-specific information on side chain environments, specifically on the changes in solvent accessibility occurring during the folding process (Kaptein 1982; Hore and Broadhurst 1993; Maeda et al. 2000; Lyon et al. 2002; Canet et al. 2003; Cemazar et al. 2003; Mok et al. 2003; Mok and Hore 2004; Mok et al. 2005, 2007). This technique therefore provides additional information on folding events. The side chain specificity of photo-CIDNP arises from the method used to produce nuclear polarization. A photochemical reaction between a suitable sensitizer molecule, usually a flavin, and an aromatic amino acid side chain generates an initially triplet-state spin-correlated radical pair, which undergoes coherent interconversion with the singlet state, modulated by hyperfine and other magnetic interactions in the radical pair. These modulations, together with the spin-selective recombination of the radical pair, result in non-Boltzmann nuclear spin populations which are observed as enhancements in the NMR spectrum of the intact protein (Kaptein 1982; Hore and Broadhurst 1993; Mok and Hore 2004). As the nuclear polarization is generated photochemically, there is no requirement to wait for nuclear spin-lattice relaxation to occur between NMR signal accumulations. The coupling of real-time NMR (Barbieri et al. 2002; Wenter et al. 2006; Furtig et al. 2007a, b; van Nuland et al. 2008) with photo-CIDNP (Hore et al. 1997; Canet et al. 2003; Schlorb et al. 2006;) allows spectra to be obtained with time-resolution limited only by the duration of the photolysis light flash ($\sim$100 ms) and the time to acquire the free induction decay (also $\sim$100 ms) (Mok and Hore 2004).

In order to generate the radical pair and hence the nuclear polarization, the amino acid side chain must be accessible to the flavin photosensitiser. Static solvent accessibility calculations can provide a guide to those residues which are exposed to the solvent, and hence have the potential to show CIDNP enhancements. The results of such calculations for the histidine and tyrosine residues,

Table 1 Static accessibility calculations for RNase A

Residue	His 12	His 48	His 105	His 119
Relative accessibility (%)[a]	8.8	0.0	34.8	57.5

Residue	Tyr 25	Tyr 73	Tyr 76	Tyr 92	Tyr 97	Tyr 115
Relative Accessibility (%)[a]	9.8	17.4	73.0	49.4	0.5	44.1

[a] Calculations were performed using the high-resolution (1.05 Å) X-ray crystallographic structure (PDB File: 1KF3 (Berisio et al. 2002)) with the Naccess program (Lee and Richards 1971; Hubbard et al. 1991). A probe radius of 1.4 Å was used throughout and the calculated accessibilities are quoted relative to that found for an extended conformation of the tripeptide Ala-Xaa-Ala, where Xaa is the residue of interest

performed using the Naccess program (Lee and Richards 1971; Hubbard et al. 1991), on a high-resolution (1.05 Å) crystal structure of RNase A at pH 5.9 (PDB file: 1KF3 (Berisio et al. 2002)), are listed in Table 1. From these data it can be seen that a number of residues are deeply buried in the native state and thus unlikely to be able to form a radical pair, and will probably not be observed in a photo-CIDNP spectrum. Of the six tyrosine residues, strong CIDNP signals can be expected from Tyr 76, Tyr 92 and Tyr 115, and, perhaps, weaker polarization from the less exposed Tyr 73. The enhancements observed in the steady-state photo-CIDNP spectrum of RNase A shown in Fig. 2, agree with these predictions and previous photo-CIDNP studies (Bolscher et al. 1979; Lenstra et al. 1979). The two tyrosine side chains that exhibit the greatest solvent accessibilities (Tyr 76 and Tyr 92) display the largest emissive peak areas (albeit overlapped due to the close proximity of their chemical shifts: 6.93 and 6.92 ppm, respectively), followed by Tyr 115 (6.81 ppm) and Tyr 73 (6.74 ppm) (Rico et al. 1989). These residues are separated into two groups: Tyr 73, Tyr 76 and Tyr 115 are clustered on the opposite side of the protein to Tyr 92 (Fig. 1). The histidine residues occur in more central locations around the substrate binding cleft, with His 105 and His 199 showing significant solvent accessibility. However, competition effects play a major complicating role in the production of photo-CIDNP in histidine residues (Winder et al. 1995). The rate constant for quenching of the triplet flavin by histidine is approximately two orders of magnitude smaller than for tyrosine and tryptophan and is also strongly dependent on the pH of the solution (Tsentalovich et al. 2002). Therefore in the presence of exposed tyrosine residues (RNase A contains no tryptophans), a histidine residue must be extremely solvent-accessible in order that it be significantly polarized. Recently, it has been shown that the accessibility of the highest occupied molecular orbital (HOMO) of the aromatic side chain gives a more robust prediction of the observation of photo-CIDNP signals, particularly in the case of limited static solvent accessibility (Khan et al. 2006). In the case of RNase A, there is little difference between the HOMO and static solvent accessibilities (data not shown).

In this paper we demonstrate the application of photo-CIDNP NMR spectroscopy to monitor the real-time refolding of RNase A triggered by rapid dilution of the chemically denatured state in either urea-d_4 or guanidine hydrochloride-d_6 (GdnDCl).

Materials and Methods

RNase A from bovine pancreas (Type XII-A) was purchased from Sigma–Aldrich (Sigma–Aldrich, Gillingham, UK) and used without further purification (purity was

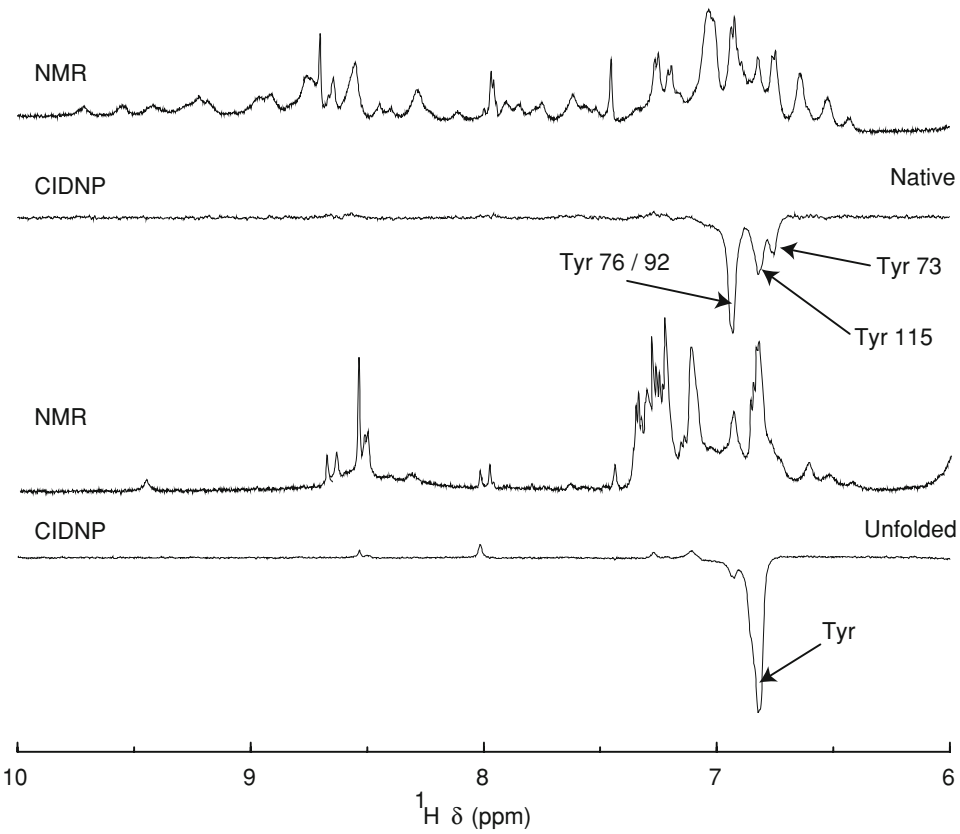

Fig. 2 Partial 600 MHz ^{1}H NMR and steady-state photo-CIDNP spectra of RNase A in 0 M (native) and 8 M (unfolded) urea-d_4, showing the amide and aromatic region. The solutions contained 2 mM RNase A, 200 μM FMN in 99.9% D_2O, and a trace of dioxane to provide a chemical shift reference at 3.75 ppm. The NMR spectra were averaged over 32 scans, while the CIDNP spectra were averaged over 16 light and dark pairs

confirmed by NMR spectroscopy). Deuterated sodium phosphate buffer, deuterated urea and GdnDCl stock solutions were prepared by three cycles of dissolution in D_2O and lyophilization. Samples were prepared in D_2O and pH adjusted using aliquots of DCl and NaOD. The pH values quoted are direct meter readings, uncorrected for the deuterium isotope effect. A trace amount of 1,4-dioxane was added to the refolding buffer as a chemical shift reference ($\delta = 3.75$ ppm). D_2O (99.8% D) was purchased from Apollo Scientific (Stockport, UK); all other chemicals were obtained from Sigma Aldrich, and were of the highest grade available.

The photo-CIDNP experiments were performed using a Varian Unity INOVA 600 spectrometer, operating at a proton frequency of 599.8 MHz, principally with a 5 mm $^1H\{^{13}C/^{15}N\}$ probe equipped with z-axis pulsed field gradients. Rapid mixing within the NMR sample tube was performed using a home-built rapid injection device, as described previously (Mok et al. 2003, 2007). The injection event was triggered using a 20 ms voltage-gated pulse from a spare TTL line on the spectrometer console. This actuated a pneumatic piston using a driving gas pressure of 10 bar. Illumination was provided by a Spectra-Physics BeamLok 2085–25S argon ion laser, usually operating at 10 W in multi-line mode (principal wavelengths 488 and 514 nm). The light was coupled to the injection device, and hence the sample, using an F-MBE optical fibre (Newport Optics) and gated into 100 ms pulses using a spectrometer-controlled LS 200 mechanical shutter (NM Laser Products). A pre-saturation pulse train was used to destroy the sample magnetisation immediately prior to each measurement. The residual solvent signal was suppressed using the CHESS (CHEmical Shift Selective) scheme (Haase et al. 1985), comprising a 2 ms selective Gaussian 90° pulse applied to the water resonance, followed by a strong field-gradient pulse to de-phase the solvent magnetisation. This procedure was repeated three times, with gradients chosen so as not to refocus the water signal. The pulse sequence is shown in Fig. 3. All NMR data was processed using the NMRPipe package (Delaglio et al. 1995).

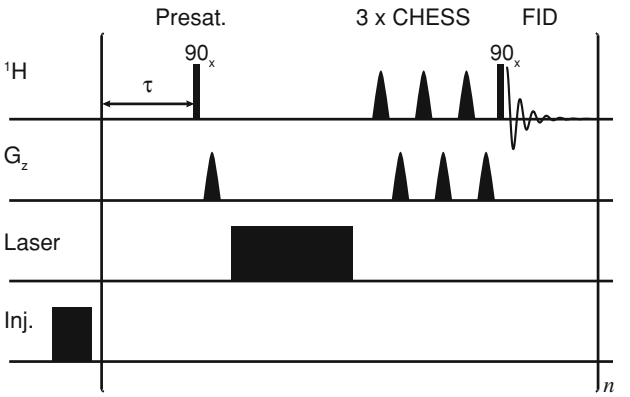

Fig. 3 The pulse sequence timing diagram for the real-time photo-CIDNP experiment. τ is a delay which can be adjusted to alter the temporal resolution of the experiment (see Main text). Inj. represents the voltage pulses used to trigger the injection device

Urea-d_4 refolding

The injection protocol used for the urea-denatured refolding experiments was as follows: a 30 μL portion of denatured protein solution (comprising 10 mM protein, 10 M urea-d_4, 100 mM sodium phosphate buffer, pH 6.0) was injected into 270 μL of refolding buffer (100 mM sodium phosphate buffer, pH 6.0) in a Shigemi NMR tube. The resulting solution contained 1 mM protein, 1 M urea-d_4, 100 mM sodium phosphate buffer, pH 6.0 after mixing; under these conditions RNase A adopts a native fold (Ahmed and Bigelow 1982). The acquisition parameters used for each of the 40 equally spaced time points were: 2,048 complex points with a spectral width of 7,005 Hz. The data sets were then extended to 4,096 complex points by forward-backward linear prediction and apodized with 2 Hz exponential line broadening prior to Fourier transformation. The spectra presented are the difference between three injections performed with illumination and three injections without illumination. These difference spectra therefore show only polarized resonances arising from the laser-induced photochemical reaction. Two sets of data were recorded spanning either 60 or 300 s in duration (i.e., one spectrum recorded every 1.5 or every 7.5 s).

NMR peak intensities as a function of the time, t, after the injection were extracted from the $\Delta t = 1.5$ s data set by Lorentzian line-fitting and globally fitted to the following equation for the signal intensity of resonance i:

$$s_i(t) = A_i \exp(-t/T_i) - A_i^{\mathrm{F}} \exp\left(-t/T^{\mathrm{F}}\right) \quad (1)$$

The refolding kinetics of peak i are characterised by an amplitude A_i, and a time constant, T_i. The second exponential term describes the decay of the signal at longer times due to photobleaching of the flavin photosensitiser (amplitude A_i^{F} and time constant T^{F}). The value of T^{F} was constrained to be the same for all resonances. Errors in the extracted parameters were estimated using Monte Carlo methods (Press et al. 1992).

Guanidine hydrochloride-d_6 refolding

For the GdnDCl denatured experiments a similar protocol was adopted: 40 μL of a 10 mM protein solution denatured in 6 M GdnDCl containing 100 mM sodium phosphate at pH 6.0 was injected into 400 μL of 100 mM sodium phosphate at pH 6.0 resulting in an 11-fold dilution. A total of 20 equally spaced spectra were recorded, spanning either 60 or 120 s ($\Delta t = 3$ s or $\Delta t = 6$ s). Time-dependent CIDNP intensities

were extracted from the spectra by Lorentzian line-fitting. Photobleaching of the flavin dye was less of a problem in these experiments so that the second exponential in Eq. (1) was not required in the fitting procedure. The CIDNP intensities for the folding intermediate were modelled with biexponential kinetics while those for the recovery of the native state Tyr 76/Tyr 92 signal were fitted to a single exponential, $s_i(t) = A_{i0} - A_{i1}\exp(-t/T_i)$ (Canet et al. 2003).

Results and discussion

Urea-d_4 refolding

Photo-CIDNP spectra obtained from the $\Delta t = 1.5$ and 7.5 s urea-d_4 refolding experiments are shown in Fig 4a and b. The initial spectrum in Fig. 4a ($t = 1.65$ s) resembles the spectrum of the fully denatured state shown in Fig. 2. Minor differences in relative peak intensities in the two spectra are attributed a small degree of refolding during the mixing dead-time. By the conclusion of the series (Fig. 4b, $t = 278$ s), the spectrum has all the features expected of the native state of RNase A, indicating that the protein has adopted its native three-dimensional fold. In the faster set of measurements (Fig. 4a), two peaks are clearly resolved: one from the overlapping resonances of Tyr 76 and Tyr 92 in the native state (~6.92 ppm) and a stronger resonance which has contributions from the unfolded state tyrosine residues and the native state Tyr 73 and Tyr 115 peaks (~6.78 ppm). The intensities of these two signals were extracted by Lorentzian line-fitting and modelled according to Eq. (1). The resulting best fits to the $\Delta t = 1.5$ s data are shown in Fig. 5. The U/Tyr 73/Tyr 115 peak shows refolding kinetics characterised by a time constant T_i of

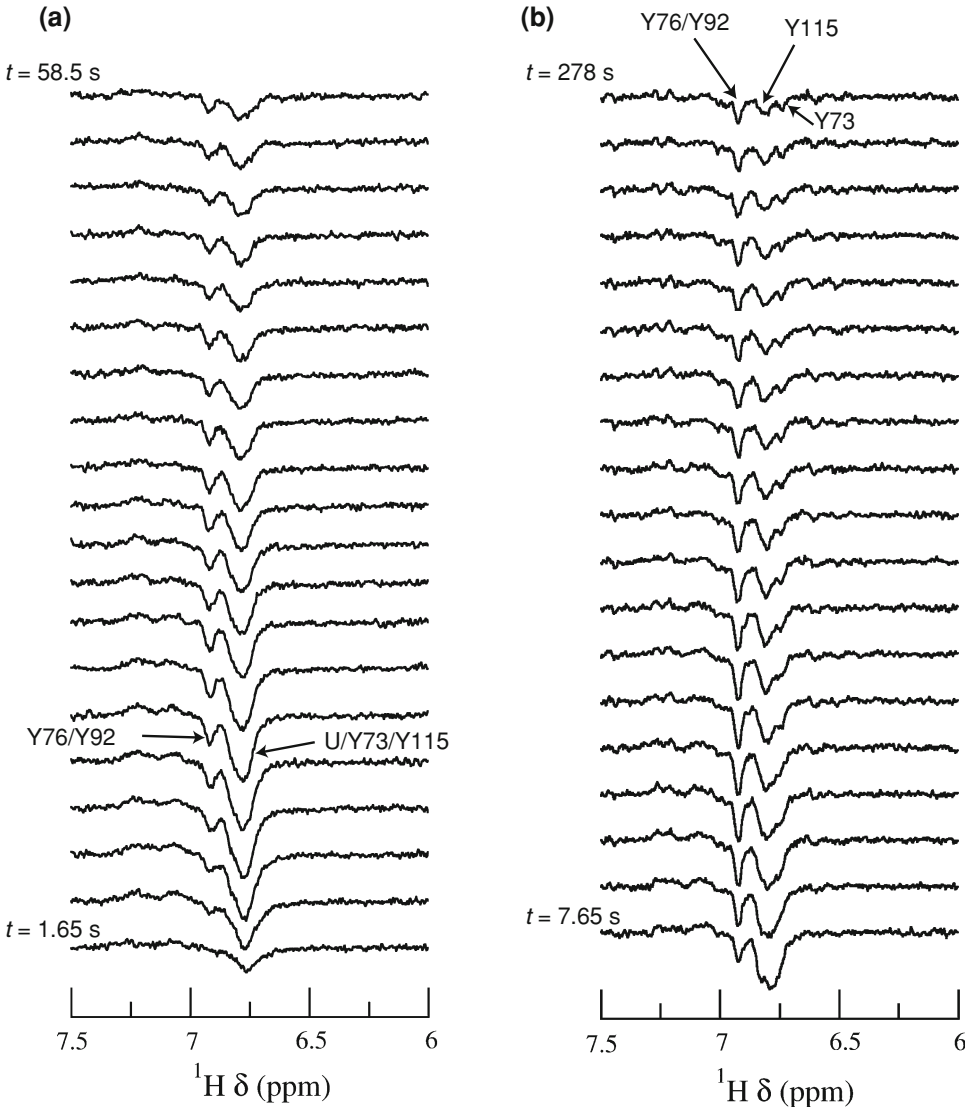

Fig. 4 Photo-CIDNP NMR spectra taken from **a** The $\Delta t = 1.5$ s and; **b** the $\Delta t = 7.5$ s urea-d_4 refolding experiments. Alternate spectra are shown. Chemical shifts were referenced to dioxane at 3.75 ppm

4.2 ± 0.2 s. This value is close to those found for the U_F species seen in single-jump stopped-flow fluorescence measurements (Houry et al. 1994) and by stopped-flow FTIR performed under similar urea-refolding conditions (Reinstädler et al. 1996). A faster folding phase (called U_{VF}; Houry et al. 1994) which occurs within the dead-time of the experiment and which in theory could be observed as a burst phase native spectral component could not be observed due to its very low population (2–6%) (Houry et al. 1994; Dodge and Scheraga 1996; Mok et al. 2003). Although the fits to the data in Fig. 5 indicate non-zero signals at $t = 0$, the estimated errors in the amplitudes A_i and A_i^F show that they are not significantly different from zero.

The overlapping Tyr 76/Tyr 92 signal at 6.92 ppm shows considerably slower recovery of native structure, with a time constant T_i of 16.6 ± 2.9 s. Biexponential fitting of the $\Delta t = 7.5$ s data (not shown) gives similar kinetics. This value shows excellent agreement with that of U_S^{II} (the slow-folding species found under urea-denaturant conditions, $\tau \sim 16$ s, (Mui et al. 1985). Hence, the discrepancy of a factor of ~4 between the measured kinetics for the two signals can be attributed to the presence of the proline residue at position 93. In the native state, this residue is found in the *cis* conformation, so that on refolding from the denatured state, in which there has been time for equilibration of *cis* and *trans* conformations, isomerization of the Tyr 92—Pro 93 peptide bond must occur before the overall native conformation can be attained. The isomerization of the X-Pro 93 *cis* peptide bond is known to be both a kinetic trap in the folding of RNase A and the origin of the I_N intermediate (Lin and Brandts 1983a, b; Biringer et al. 1988; Bhat et al. 2003).

A further feature of the refolding data is the photoreduction of the FMN photosensitiser which superimposes a decay term onto the protein folding kinetics (Maeda et al. 2000; Mok et al. 2003). This is observable in Fig. 4 as a progressive attenuation the intensities of the later spectra in each series. The decay arises because the photochemically formed flavin semiquinone radical undergoes a disproportionation reaction, regenerating the original flavin and producing the colourless fully reduced flavin hydroquinone which is unreactive in the CIDNP experiment (Müller 1991; Maeda et al. 2000). The time constant T^F observed for this process (36.4 s, Fig. 5) is comparable to those reported previously (Maeda et al. 2000). The effects of photobleaching are satisfactorily treated by means of a single time constant for the two polarized resonances, indicating that the protein itself is not involved in this process.

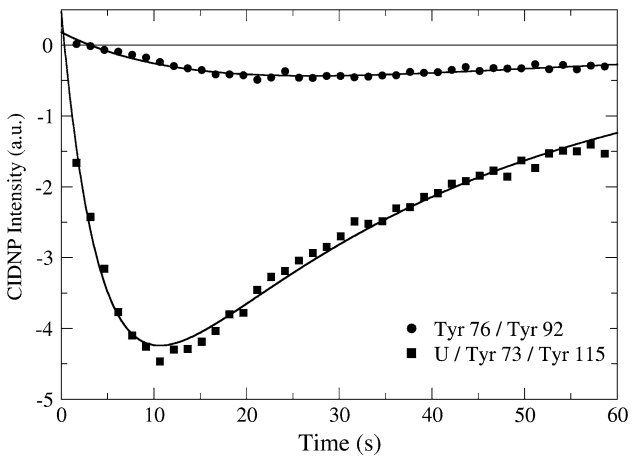

Fig. 5 Measured CIDNP intensities plotted as a function of time after the initiation of refolding from urea-d_4. The solid lines are the best fits to Eq. (1)

Guanidine hydrochloride-d_6 refolding

Real-time photo-CIDNP spectra obtained from the GdnDCl refolding experiments are shown in Fig. 6. The initial spectrum, acquired 3.8 s after the injection, is very similar to the unfolded state photo-CIDNP spectrum shown in Fig. 2. Once again, there are minor differences in the observed relative intensities arising from the folding that occurs during the mixing dead-time. At the conclusion of this series, the spectrum is again characteristic of the RNase A native state, demonstrating that the protein has refolded correctly. These spectra show strong similarity to those obtained from the urea-refolding experiments. However, there are two distinct differences: a weak adsorptively polarized resonance at 7.08 ppm corresponding to His119 and a non-native emissive signal at approximately 6.85 ppm. The time dependence of the photo-CIDNP intensities from both sets of data ($\Delta t = 3$ s and $\Delta t = 6$ s) are shown in Fig. 7. The value of T_i for the native state Tyr 76/Tyr 92 peak obtained by single-exponential fitting, is 7.6 ± 1.4 s. The signal at 6.85 ppm does not correspond to the chemical shift of any of the tyrosine residues in native RNase A, indicating that it arises from an intermediate formed on the folding pathway. This peak shows biexponential behaviour, appearing with a time constant of 7.3 ± 1.1 s and subsequently decaying with a time constant of 24.0 ± 2.3 s. The latter is in excellent agreement with various single-jump refolding experiments performed in GdnHCl reported by the Scheraga laboratory: wild-type, $\tau = 22.8$ s (Houry et al. 1994) and $\tau = 30$ s (Dodge and Scheraga 1996), and the single tryptophan mutant Y92 W, $\tau = 22.5$ s (Sendak et al. 1996). In all cases, the values of the time constants suggest that this signal arises from Tyr 92 in the native-like intermediate I_N species known to be formed on the U_S^{II} slow folding pathway. As in the urea-refolding case, the small non-zero amplitudes of the fits at $t = 0$ are not significant.

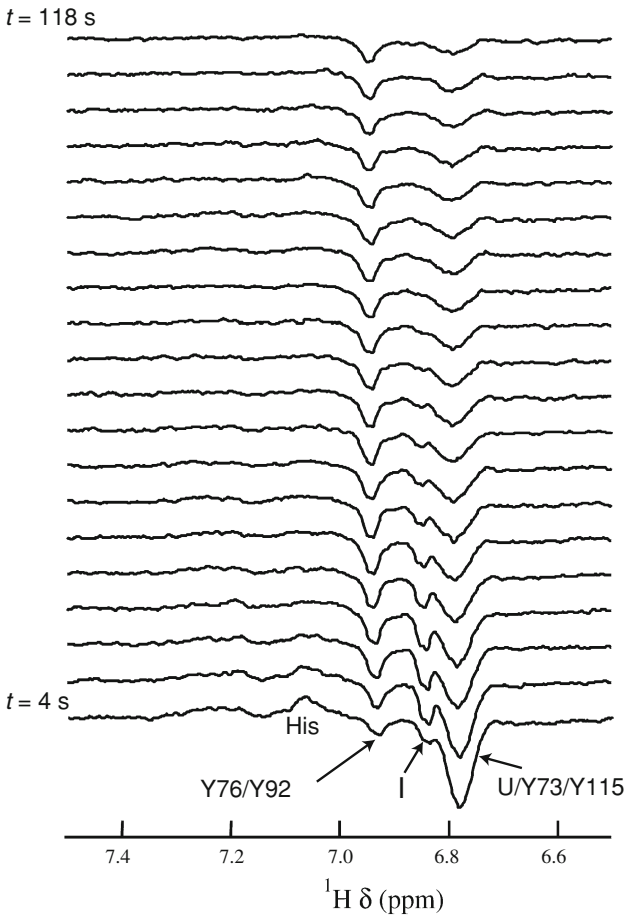

Fig. 6 Photo-CIDNP NMR spectra taken from the GdnDCl refolding experiments ($\Delta t = 6$ s data series). Chemical shifts were referenced to dioxane at 3.75 ppm

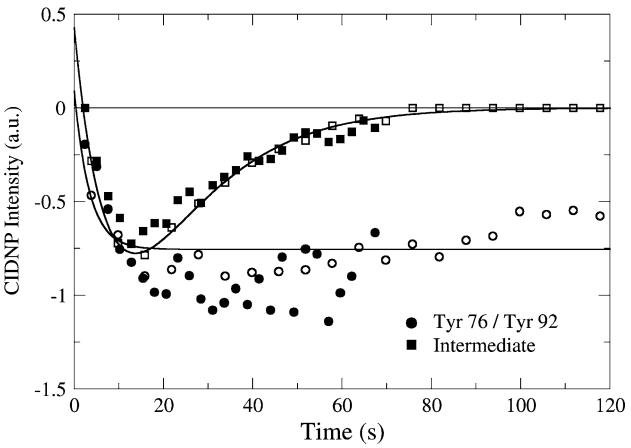

Fig. 7 Measured CIDNP intensities plotted as a function of time after the initiation of refolding from GdnDCl. Filled and open symbols refer to the $\Delta t = 3$ s and $\Delta t = 6$ s data sets, respectively. The solid lines are the best fits (see text for details)

The GdnDCl refolding results are do not appear to be affected by photobleaching of the flavin dye in contrast to the urea-d_4 refolding experiments. The origin of this difference is unclear.

Comparison of refolding experiments

In general, rather similar results are obtained for the refolding of RNase A denatured using either urea or GdnDCl monitored by photo-CIDNP NMR spectroscopy. Two distinct kinetic processes are apparent, a faster step with time constant of 4–8 s (4.2 s in urea and 7.3/7.6 s in GdnDCl) and a slower one with time constant 16–24 s (16.6 s in urea and 24.0 s in GdnDCl). The latter is attributed to the *cis-trans* isomerization of Pro 93 and is responsible for the slow disappearance of the signal from Tyr 92 in the folding intermediate observed in the GdnDCl experiment. The similarity of the rise times of this resonance (7.3 s) and that of the native tyrosine peak at 6.92 ppm (7.6 s) in GdnDCl is consistent with the formation at similar rates of the native state from unfolded states containing cis-Pro 93 and of the intermediate state from unfolded states containing trans-Pro 93. The slower refolding time constant (~ 17 s) observed for the Tyr76/Tyr 92 peak in urea arises from the superposition of the resonances of these two native state residues with that of Tyr-92 in the intermediate whose slower refolding and strong polarization evidently determines the observed kinetics. Tyr 92, whose accessibility changes more than that of Tyr 76 on refolding from a completely unfolded state (Table 1), can be expected to dominate the observed kinetics when, as in urea, the intermediate and native Tyr 92 chemical shifts cannot be resolved. Overall, the measured time constants indicate that both experiments probe the same refolding reaction and the same portion of the folding landscape (Mui et al. 1985). The extracted time constants are also in good agreement with literature values reported by others (Houry et al. 1994; Dodge and Scheraga 1996; Sendak et al. 1996).

An intriguing difference, however, is that the distinct signal arising from an intermediate state is only seen in the case of refolding from GdnDCl. The appearance of this non-native Tyr signal exclusively in GdnDCl-refolding has not been observed before with other techniques, and it had been suggested that the refolding of RNase A from urea- and GdnHCl-denatured states proceeds through highly similar pathways (Mui et al. 1985). One possible reason for this discrepancy is the very different ionic strengths in the two experiments: GdnDCl, being ionic, results in a much larger ionic strength than urea-d_4. To probe the effect of this difference, urea-d_4 refolding experiments were performed using a larger concentration of sodium phosphate buffer, around 1 M, to increase the ionic strength of the refolding solution. Under these conditions, a small signal at the position of the proposed I_N intermediate species is observed (data not shown), indicating that the ionic strength of the refolding reaction solution is sufficient to produce the change in chemical shift needed to allow Tyr 92 to be detected with the time-resolved CIDNP methodology.

The native structure of RNase A contains two proline residues in the *cis*-conformation (Tyr 92-Pro 93 and Asn 113-Pro 114) and two in the *trans*-conformation (Lys 41-Pro 42 and Val1 16-Pro 117). In addition to probing the solvent-accessibilities of tyrosine side chains in real time while a protein refolds (Hore et al. 1997; Maeda et al. 2000; Wirmer et al. 2001; Mok et al. 2003; Canet et al. 2003), our methodology provides further information on tyrosine side chains that are sequence-wise proximal to proline residues—in particular Tyr 92 for RNase A. In other words, depending on the microscopic environment of these tyrosine side chains as influenced by the *cis-trans* isomeric state of the proline (and provided that there is reasonable chemical shift dispersion), monitoring of kinetically different populations en route to the native state would be possible through the photo-CIDNP of Tyr 92 and/or Tyr 115. We observe this for Tyr 92 in both urea- and GdnDCl-refolding experiments. In the urea-refolding case, the refolding time constant extracted from the overlapping Tyr 76/Tyr 92 resonances agree well with the U_S species (Fig. 4) (Dodge and Scheraga 1996). Noting that the natively highly-accessible Tyr 76 has been found to be relatively uninvolved in stabilizing the native structure and unimportant in influencing various stopped-flow spectroscopic folding experiments (Sendak et al. 1996; Juminaga et al. 1997), we infer that the time-dependence of the Tyr 76/Tyr 92 peak is mainly that of Tyr 92, hence providing a *cis-trans* isomerism probe for the adjacent Pro 93. In the GdnDCl-refolding case (Fig. 6), the appearance and then disappearance of the non-native intermediate signal provides even stronger evidence for the involvement of Pro 93 as manifested through Tyr 92, since the kinetics of Tyr 76 are now independently shown to be in agreement not with the U_S species, but with the U_F species. The biexponential kinetics of the non-native intermediate peak (Fig. 6, 7) strongly suggest that the build-up of the native structure proceeds in a parallel manner, and not sequentially.

A variety of sub-millisecond, ultra-rapid mixing techniques coupled with fluorescence, circular dichroism, or small-angle X-ray scattering detection methods has shown that the initial burst-phase signal classically present in the folding of RNase A belongs to a specific folding-related structural rearrangement (Welker et al. 2004; Kimura et al. 2005), and not merely a rearrangement of the unfolded state as a result of changing solvent conditions (Qi et al. 1998). Due to the global nature of the optical spectroscopic/X-ray scattering signals, most of these modern methods require continuous-flow (or double-jump stopped-flow if utilizing classical procedures) to ensure that the natively-*cis* Pro residues are not allowed to equilibrate with their *trans* isomers in the unfolded state. In contrast, despite having a time resolution more than an order of magnitude slower, real-time photo-CIDNP spectroscopy is nevertheless able to detect and partially-resolve subtle non-native *cis-trans* isomerized species. In other words, the sensitivity of real-time NMR coupled with photo-CIDNP appears to permit the simultaneous detection of multiple isomerized populations during the folding reaction. Although the relatively large number of Tyr side chains in RNase A has prevented a clear distinction of the isomeric populations or the determination of their individual kinetics, work on other proteins such as lysozyme, α-lactalbumin, and HPr has shown that even with several accessible aromatic residues, monitoring of individual Trp, Tyr, or His side chains by time-resolved, ^{1}H photo-CIDNP is a powerful method of probing the folding process (Hore et al. 1997; Maeda et al. 2000; Canet et al. 2003; Cemazar et al. 2003; Mok et al. 2003; Mok and Hore 2004; Mok et al. 2007).

Conclusions

The refolding of disulfide-intact RNase A has been studied extensively using numerous methods (Neira and Rico 1997; Raines 1998; Chatani and Hayashi 2001), amongst others, stopped-flow circular dichroism and fluorescence, enzymatic activity, limited proteolysis (Lin and Brandts 1983a, b), quench-flow H/D exchange with or without NMR (Udgoankar and Baldwin 1988), and time-resolved FTIR (Reinstädler et al. 1996). Site-directed mutagenesis is often employed in conjunction with the above techniques to provide further information on the roles of individual amino acid residues in the refolding mechanism (Chatani and Hayashi 2001). A study of single alanine-substituted mutants of the four proline residues of RNase A shows that *cis-trans* isomerism of the Tyr 92—Pro 93, Ala 113—Pro 114, and Val 116—Pro 117 peptide bonds is strongly involved in the kinetics of refolding *en route* to the native state, resulting in a "box"-shaped model for the mechanism of unfolding/refolding of RNase A (Dodge and Scheraga 1996). The photo-CIDNP methodology employed here allows us to monitor sensitively the local structural changes of one of the above three proline isomerizations through the observation of the H3,5 peak of Tyr 92, appearing as an emissive signal in the CIDNP experiment. The methodology we describe in this paper does not require site-directed substitutions, which need careful prior verification to establish the equivalence of the mutants with the wild type in terms of three-dimensional structure, enzymatic activity, and thermodynamic stability (Schultz and Baldwin 1992).

Real-time photo-CIDNP NMR provides information on the changes in the solvent accessibilities of aromatic side chains (tyrosines in the case of RNase A) as a function of time (Hore et al. 1997; Maeda et al. 2000; Canet et al.

2003; Cemazar et al. 2003; Mok et al. 2003; Mok and Hore 2004; Mok et al. 2007). Due to the laser-induced generation of nuclear polarization, it is possible to sample closely spaced time points, without the need to wait for nuclear spin-lattice relaxation between signal acquisitions. Whereas optical spectroscopic methods report on global folding changes, provided that there is sufficient chemical shift resolution the detection and investigation of individual side chain protons is feasible with real-time photo-CIDNP NMR. As a result, one can monitor local structural changes, providing significant insights into protein folding at a residue-specific level. This allows information to be used in computational models where comparison with experimental results on an atomic level serves as a helpful benchmark, and allows validation of the models. The work described in this paper shows the utility of the real-time photo-CIDNP methodology and its application to the study of the folding properties of proteins.

Acknowledgments We thank Elizabeth Sutton for preliminary experiments and Dr Ilya Kuprov for calculating the HOMO accessibilities. We acknowledge a UK Foreign and Commonwealth Office Chevening Scholarship (to KHM), and financial support from the BBSRC and INTAS.

References

Ahmed F, Bigelow CC (1982) Estimation of the stability of ribonuclease A, lysozyme, α-lactalbumin, and myoglobin. J Biol Chem 21:12935–12938

Anfinsen CB (1973) Principles that govern the folding of protein chains. Science 181:223–230

Barbieri R, Hore PJ, Luchinat C, Pierattelli R (2002) An NMR method for studying the kinetics of metal exchange in biomolecular systems. J Biomol NMR 23:303–309

Berisio R, Sica F, Lamzin VS, Wilson KS, Zagari A, Mazzarella L (2002) Atomic resolution structures of ribonuclease A at six pH values. Acta Cryst D58:441–450

Bhat R, Wedemeyer WJ, Scheraga HA (2003) Proline isomerization in bovine pancreatic ribonuclease A. 2. folding conditions. Biochemistry 42:5722–5728

Biringer RG, Austin CM, Fink AL (1988) Intermediates in the folding of ribonuclease at subzero temperature 2: monitoring by inhibitor binding and catalytic activity. Biochemistry 27:311–315

Bolscher BGJM, Lenstra JA, Kaptein R (1979) Accessibility of aromatic residues of bovine pancreatic ribonuclease as revealed by laser photo-CIDNP. J Magn Reson 35:163–166

Canet D, Lyon CE, Scheek RM, Robillard GT, Dobson CM, Hore PJ, van Nuland NAJ (2003) Rapid formation of non-native contacts during the folding of HPr revealed by real-time photo-CIDNP NMR and stopped-flow fluorescence experiments. J Mol Biol 350:397–407

Cemazar M, Zahariev S, Lopez JJ, Carugo O, Jones JA, Hore PJ, Pongor S (2003) Oxidative folding intermediates with non-native disulphide bridges between adjacent cysteine residues. Proc Natl Acad Sci USA 100:5754–5759

Chatani E, Hayashi R (2001) Functional and structural roles of constituent amino acid residues of bovine pancreatic ribonuclease A. J Biosci Bioeng 92:98–107

Delaglio F, Grzesiek S, Vuister GW, Zhu G, Pfeifer J, Bax A (1995) NMRPipe: a multidimensional spectral processing system based on UNIX pipes. J Biomol NMR 6:277–293

Dobson CM (2003) Protein folding and misfolding. Nature 426: 884–890

Dodge RW, Scheraga HA (1996) Folding and unfolding kinetics of the proline-to-alanine mutants of bovine pancreatic ribonuclease A. Biochemistry 35:1548–1559

Furtig B, Wenter P, Reymond L, Richter C, Pitsch S, Schwalbe H (2007a) Conformational dynamics of bistable RNAs studied by time-resolved NMR spectroscopy. J Am Chem Soc 129: 16222–16229

Furtig B, Buck J, Manoharan V, Barmel W, Jaschke A, Wenter P, Pitsch S, Schwalbe H (2007b) Time-resolved NMR studies of RNA folding. Biopolymers 86:360–383

Gahl RF, Narayan M, Xu G, Scheraga HA (2008) Dissimilarity in the oxidative folding of onconase and ribonuclease A, two structural homologues. Protein Eng Des Sel 21:223–231

Haase A, Frahm J, Hänicke W, Matthaei D (1985) ^{1}H NMR chemical shift (CHESS) selective imaging. Phys Med Biol 30:341–344

Hore PJ, Broadhurst RW (1993) Photo-CIDNP of biopolymers. Prog NMR Spec 25:345–402

Hore PJ, Winder SL, Roberts CH, Dobson CM (1997) Stopped-flow photo-CIDNP observation of protein folding. J Am Chem Soc 119:5049–5050

Houry WA, Rothwarf DM, Scheraga HA (1994) A very fast folding phase in the refolding of disulphide-intact ribonuclease A: implications for the refolding and unfolding pathways. Biochemistry 33:2516–2530

Hubbard SJ, Campbell SF, Thornton JM (1991) Molecular recognition: conformational analysis of limited proteolytic sites and serine proteinase protein inhibitors. J Mol Biol 220:507–530

Juminaga D, Wedemeyer WJ, Garduno-Juarez R, McDonald MA, Scheraga HA (1997) Tyrosyl interactions in the folding and unfolding of bovine pancreatic ribonuclease A: a study of tyrosine-to-phenylalanine mutants. Biochemistry 36:101331–110145

Kaptein R (1982) Photo-CIDNP studies of proteins. In: Berliner LJ, Reubens J (eds) Biological magnetic resonance, vol 4. Plenum Press, New York, pp 145–191

Khan F, Kuprov I, Craggs TD, Hore PJ, Jackson SE (2006) ^{19}F NMR studies of the native and denatured states of green fluorescent protein. J Am Chem Soc 128:10729–10737

Kimura T, Akiyama S, Uzawa T, Ishimori K, Morishiima I, Fujisawa T, Takahashi S (2005) Specifically collapsed intermediate in the early stage of the folding of ribonuclease A. J Mol Biol 350: 349–362

Koradi R, Billeter M, Würtrich K (1996) MOLMOL: a program for display and analysis of macromolecular structures. J Mol Graphics 14:51–55

Lee B, Richards FM (1971) The interpretation of protein structures: estimation of static accessibilities. J Mol Biol 55:379–400

Lenstra JA, Bolscher BGJM, Stob S, Beintema JJ, Kaptein R (1979) The aromatic residues of bovine pancreatic ribonuclease studied by ^{1}H nuclear magnetic resonance. Eur J Biochem 98:385–397

Lin L, Brandts JF (1983a) Determination of *cis-trans* proline isomerisation by trypsin proteolysis: applications to a model pentapeptide and to oxidised ribonuclease A. Biochemistry 22:553–559

Lin L, Brandts JF (1983b) Isomerism of Proline-93 during the unfolding and refolding of ribonuclease A. Biochemistry 22:559–563

Lyon CE, Suh E-S, Dobson CM, Hore PJ (2002) Probing the exposure of tyrosine and tryptophan residues in partially folded proteins and folding intermediates by CIDNP pulse labelling. J Am Chem Soc 124:13018–13024

Maeda K, Lyon CE, Lopez JJ, Cemazar M, Dobson CM, Hore PJ (2000) Improved photo-CIDNP methods for studying protein structure and folding. J Biomol NMR 16:235–244

Mok KH, Hore PJ (2004) Photo-CIDNP NMR methods for studying protein folding. Methods 34:75–87

Mok KH, Nagashima T, Day IJ, Jones JA, Jones CJV, Dobson CM, Hore PJ (2003) Rapid sample-mixing technique for transient NMR and photo-CIDNP spectroscopy: applications to real-time protein folding. J Am Chem Soc 125:12484–12492

Mok KH, Nagashima T, Day IJ, Hore PJ, Dobson CM (2005) Multiple subsets of side-chain packing in partially folded states of α-Lactalbumins. Proc Natl Acad Sci USA 102:8899–8904

Mok KH, Kuhn LT, Goez M, Day IJ, Lin JC, Andersen NH, Hore PJ (2007) A pre-existing hydrophobic collapse in the unfolded state of an ultrafast folding protein. Nature 447:106–109

Mui PW, Konishi Y, Scheraga HA (1985) Kinetics and mechanism of the refolding of denatured ribonuclease A. Biochemistry 24:4481–4489

Müller F (1991) Free flavins: synthesis, chemical and physical properties. In: Müller F (ed) The chemistry and biochemistry of flavins, 1st edn. CRC Press, Boca Raton, pp 1–71

Narayan M, Welker E, Wedemeyer WE, Scheraga HA (2000) Oxidative folding of proteins. Acc Chem Rev 33:805–812

Neira JL, Rico M (1997) Folding studies on ribonuclease A, a model protein. Folding and Design 2:R1–R11

Press WH, Flannery BP, Teukolsky SA, Vetterling WT (1992) Numerical Recipes in FORTRAN 77. Cambridge University Press, Cambridge

Qi PX, Sosnick TR, Englander SW (1998) The burst phase in ribonuclease A folding and solvent dependence of the unfolded state. Nat Struct Biol 5:882–884

Raines RT (1998) Ribonuclease A. Chem Rev 98:1045–1065

Reinstädler D, Fabian H, Backmann J, Naumann D (1996) Refolding of thermally and urea-denatured ribonuclease A monitored by time-resolved FTIR spectroscopy. Biochemistry 35:15822–15830

Rico M, Bruix M, Santoro J, Gonzalez C, Neira JL, Nieto JL, Herranz J (1989) Sequential ^{1}H-NMR assignments and solution structure of bovine pancreatic ribonuclease A. Eur J Biochem 183:623–638

Sambashivan S, Liu Y, Sawaya MR, Gingery M, Eiseberg D (2005) Amyloid-like fibrils of ribonuclease A with three-dimensional domain-swapped and native-like structure. Nature 437:266–269

Santoro J, Gonzàlez C, Bruix M, Neira JL, Neito JL, Herranz J, Rico M (1993) High-resolution three-dimensional structure of Ribonuclease A in solution by nuclear magnetic resonance spectroscopy. J Mol Biol 229:722–734

Saunders M, Wishnia A, Kirkwood JG (1957) The nuclear magnetic resonance spectrum of ribonuclease. J Am Chem Soc 79:3289–3290

Schlorb C, Mensch S, Ritcher C, Schwalbe H (2006) Photo-CIDNP reveals differences in compaction of non-native states of lysozyme. J Am Chem Soc 128:1802–1803

Schultz DA, Baldwin RL (1992) *Cis* proline mutants of ribonuclease A I. Thermal stability. Protein Sci 1:910–916

Schultz DA, Schmid FX, Baldwin RL (1992) *Cis* proline mutants of ribonuclease A II. Elimination of the slow-folding forms by mutation. Protein Sci 1:917–924

Sendak RA, Rothwarf DM, Wedemeyer WJ, Houry WA, Scheraga HA (1996) Kinetic and thermodynamic studies of a tryptophan-containing mutant of ribonuclease A. Biochemistry 35:12978–12992

Tsentalovich YuP, Lopez JJ, Hore PJ, Sagdeev RZ (2002) Mechanisms of reactions of flavin mononucleotide triplet with aromatic amino acids. Spectrochim Acta A 58:2043–2050

Udgaonkar JB, Baldwin RL (1988) NMR evidence for an early framework intermediate on the folding pathway of ribonuclease A. Nature 335:694–699

van Nuland NA, Dobson CM, Regan L (2008) Characterization of folding the four-helix bundle protein Rop by real-time NMR. Protein Eng Des Sel 21:165–170

Wedemeyer WJ, Welker E, Narayan M, Scheraga HA (2000) Disulfide bonds and protein folding. Biochemistry 39:4207–4216

Welker E, Maki K, Shastry MCR, Juminaga D, Bhat R, Scheraga HA, Roder H (2004) Ultrarapid mixing experiments shed new light on the characteristics of the initial conformational ensemble during the folding of ribonuclease A. Proc Natl Acad Sci USA 101:17681–17686

Wenter P, Furtig B, Hainard A, Schwalbe H, Pitsch S (2006) A caged uridine for the selective preparation of an RNA fold and determination of its refolding kinetics by real-time NMR. Chembiochem 7:417–420

Winder SL, Broadhurst RW, Hore PJ (1995) Photo-CIDNP of amino acids and proteins: effects of competition for flavin triplets. Spectrochim Acta A 51:1753–1761

Wirmer J, Kühn T, Schwalbe H (2001) Millisecond time resolved photo-CIDNP NMR reveals a non-native folding intermediate on the ion-induced refolding pathway of bovine alpha-lactalbumin. Angew Chem Int Ed 40:4248–4251